Nonlinear Viscoelastic Modeling of Finger Arteries: Toward Smartphone-Based Blood Pressure Monitoring via the Oscillometric Finger Pressing Method

Cederick Landry, Mark Freithaler, Vishaal Dhamotharan, Hadi Daher, Sanjeev G. Shroff, and Ramakrishna Mukkamala

Abstract*—*Objective: **Oscillometric finger pressing is a smartphone-based blood pressure (BP) monitoring method. Finger photoplethysmography (PPG) oscillations and pressure are measured during a steady increase in finger pressure, and an algorithm computes systolic BP (SP) and diastolic BP (DP) from the measurements. The objective was to assess the impact of finger artery viscoelasticity on the BP computation. *Methods:* Nonlinear viscoelastic models relating transmural pressure (finger BP – applied pressure) to PPG oscillations during finger pressing were developed. The output of each model to a measured transmural pressure input was fitted to measured PPG oscillations from 15 participants. A parametric sensitivity analysis was performed via model simulations to elucidate the viscoelastic effect on the derivative-based BP computation algorithm. *Results:* A Wiener viscoelastic model comprising a first-order transfer function followed by a static sigmoidal function fitted the measured PPG oscillations better than an elastic model containing only the static function (median (IQR) error of 30.5% (25.6%-34.0%) vs 50.9% (46.7%-53.7%); $p<0.01$). In Wiener model simulations, the derivative algorithm underestimated SP, especially with high pulse pressure and low transfer function cutoff frequency (i.e., greater viscoelasticity). The mean of the normalized PPG waveform at the maximum oscillation beat was found to correlate with the cutoff frequency ($r = -0.8$) and could thus possibly be used to compensate for viscoelasticity. *Conclusion:* Finger artery viscoelasticity negatively impacts oscillometric BP computation algorithms but can potentially be compensated for using available measurements. *Significance:* These findings may help in converting smartphones into truly cuffless BP monitors for improving hypertension awareness and control.**

***Index Terms*—Arterial viscoelasticity, blood pressure computation, cuffless blood pressure, finger arteries, force sensing, mHealth, nonlinear dynamic model, oscillometric finger pressing, photoplethysmography (PPG), system identification.**

I. Introduction

Ubiquitous blood pressure (BP) monitoring via readily available smartphones may improve hypertension awareness and control rates, which are low worldwide [1]. Oscillometric finger pressing is a cuffless and calibration-free BP monitoring method that leverages the oscillometric principle (principle behind most automated cuff devices) to turn smartphones into BP measurement tools [2], [3].

As described in [4], the oscillometric principle measures BP by exploiting the sigmoidal relationship between blood volume and transmural pressure in arteries, where transmural pressure is the internal BP minus the external pressure. It involves gradually changing the external pressure on an artery (and thus the transmural pressure) to first increase and then decrease the blood volume oscillation amplitude and using an algorithm to compute BP from the blood volume oscillation amplitude versus external pressure function ("oscillogram"). Traditional devices slowly inflate or deflate a cuff over the brachial artery to vary its external pressure and measure the pressure waveform inside the cuff to extract both the external pressure via lowpass filtering and the variable-amplitude blood volume oscillations via highpass filtering. In the oscillometric finger pressing method, the user serves as the actuator instead of the cuff by slowly pressing their fingertip against a smartphone to increase the external pressure of the underlying artery, while the phone acts as the sensor rather than the cuff device by employing an embedded photoplethysmography (PPG)-force sensor unit to record the resulting variable-amplitude blood volume oscillations and applied finger pressure, respectively. An algorithm is then likewise used to compute systolic and diastolic BP (SP and DP) from the oscillogram. To date, no accurate algorithm to compute BP from the raw fingertip measurements does not exist.

We have previously employed a purely elastic model of the finger artery, wherein arterial transmural pressure and volume are related by a sigmoidal function [4], to make predictions on finger oscillometric measurements, and have developed and evaluated different model-based algorithms to compute BP from these measurements [5]. However, we observed a tendency for underestimation of pulse pressure (PP) in our experiments, which was not predicted by the model [5], [6].

This work was supported by the NIH Grants HL146470 and HL076124 and the NSERC PDF 568003–2022.

C. Landry, M. Freithaler, H. Daher, V. Dhamotharan, and S. G. Shroff are with the Department of Bioengineering, University of Pittsburgh, Pittsburgh, PA, USA.

R. Mukkamala is with the Departments of Bioengineering and Anesthesiology and Perioperative Medicine, University of Pittsburgh, Pittsburgh, PA (email: rmukkamala@pitt.edu)

It has been shown that small finger arteries do not exhibit purely elastic or static behavior but rather viscoelastic or dynamic behavior (e.g., arterial blood volume increases slowly instead of instantaneously to a step increase in transmural pressure) as indicated by hysteresis loops in plots of measured arterial volume versus transmural pressure [7]. It was also shown that finger artery viscoelastic effects increase with smooth muscle contraction. Moreover, smooth muscle contraction is known to vary acutely over time. So, finger artery viscoelasticity could be a nontrivial source of error for oscillometric BP computation algorithms based on purely elastic models and the cause of our PP underestimation observation.

In this study, we conducted nonlinear viscoelastic modeling in the context of the oscillometric finger pressing method. We quantified the extent of viscoelasticity by fitting viscoelastic and purely elastic models to finger oscillometric measurements. We found that finger artery viscoelasticity cannot be ignored. We then performed a model parametric sensitivity analysis to reveal the adverse impact of viscoelasticity on a popular elastic model-based oscillometric BP computation algorithm. Finally, we proposed a potential remedy toward accurately computing BP despite the finger viscoelastic effect.

II. Methods

A. Data Collection for Model Building

Physiologic data were collected from 15 healthy participants under IRB approval and with written, informed consent (STUDY20060267, 2020 –). The participant demographics were as follows: 33% female, 31±12 (mean±standard deviation) years of age, 75±11 kg in weight, and 172±8 cm in height. A custom benchtop system, detailed in [5], consisting of an infrared reflectance-mode PPG sensor on top of a load cell was utilized to measure finger arterial volume oscillations and applied pressure, as shown in Fig. 1. The PPG and applied pressure data were collected at 1000 Hz using a commercial data acquisition unit (USB-6003, NI). The participants were guided with visual feedback on a monitor to linearly increase finger pressure over time. Each participant performed the finger pressing method while holding the sensor-unit at heart level. A finger arterial BP waveform was recorded simultaneously via a finger cuff volume-clamp device (NOVA, Finapres) at 200 Hz, as also shown in Fig. 1. Electrodes in lead I configuration were used to record an ECG waveform via the NOVA and the NI analog inputs for synchronization purposes. The collected data were down sampled to 100 Hz for further analysis.

B. Model Input and Output

The finger artery system for identification relates the transmural pressure ($P_T(t)$) to the blood volume in the artery ($V(t)$). $P_T(t)$ of an artery, defined as the internal BP ($P_a(t)$) minus the external pressure ($P_e(t)$), is measured in the experimental setup (Fig. 1). While absolute blood volume cannot be measured, PPG can measure a waveform proportional to the arterial blood volume oscillations ($PPG_{ac}(t)$). The PPG_{ac} waveform is therefore a highpass filtered version of $V(t)$ multiplied by an unknown constant (k). The identifiable system thus comprises the nonlinear dynamics of the artery in cascade with the highpass filter and PPG scaling, as shown in Fig. 2, where $P_T(t)$ is the input and $PPG_{ac}(t)$ is the output of the

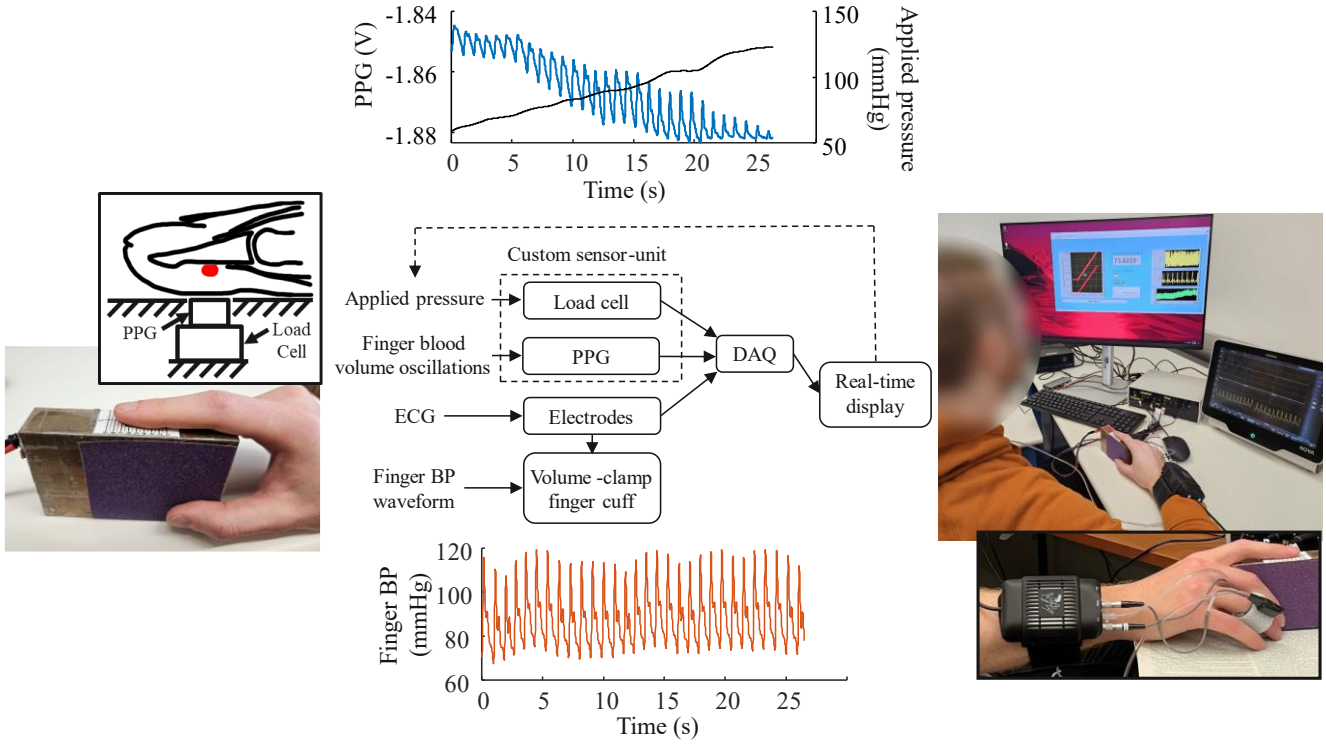

Fig. 1. Devices and data collection. Custom benchtop system including an infrared reflectance-mode photoplethysmography (PPG) sensor above a load cell (left) for recording finger blood volume oscillations and applied pressure (upper center). Visual feedback via a real-time display for guiding the user to linearly increase finger pressure over time while maintaining the hand at heart level (right). Finger cuff volume-clamp device (right) for obtaining a finger blood pressure (BP) waveform (lower center). Block diagram of overall system (center).

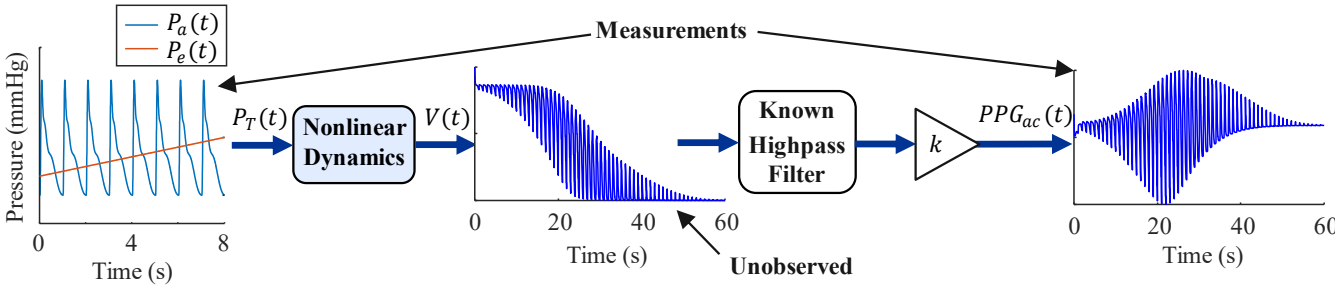

Fig. 2. The finger artery system for identification relating transmural pressure ($P_T(t)$) to blood volume ($V(t)$). Transmural pressure equals the finger BP waveform ($P_a(t)$) minus the finger external pressure ($P_e(t)$) and is measured. $V(t)$ cannot be measured. The system is thus identified from the measured blood volume oscillations ($PPG_{ac}(t)$), which is related to $V(t)$ through a known highpass filter and an unknown scale factor (k), as well as $P_T(t)$.

system. The highpass filter is known and the same as the one used for filtering the raw PPG measurements (first order Butterworth filter with cutoff frequency of 0.3 Hz). Essentially, only the nonlinear dynamic model (as well as the PPG scaling) is identified from $P_T(t)$ and $PPG_{ac}(t)$.

The following assumptions were made for the model input. The finger BP waveform measured via the volume-clamp device is accurate in shape and peak-to-peak amplitude and reflects the actual BP dynamics of the finger artery. BP at the digital arteries of the middle finger's middle phalanx is the same as BP at the transverse palmar arch artery of the pointer finger's fingertip. Finally, BP is not affected by the compression of the artery – a standard assumption in oscillometry.

C. *Viscoelastic and Elastic Models*

A Hammerstein model (static nonlinearity followed by linear dynamics) and a Wiener model (linear dynamics followed by static nonlinearity) were employed to represent arterial nonlinear viscoelasticity. These models are typical representations of nonlinear dynamics that are often encountered in biological systems and are easily identifiable [8]. Although they may be part of the black-box model family, they were quite interpretable models here, since they were designed with knowledge of arterial physiology. In particular, the static nonlinearity in both models is a sigmoidal function, which is known to enable good fitting of oscillometric arm cuff measurements and has parameters that carry physiological meaning [4]. The impact of the difference in the structural order of the static nonlinearity and linear dynamics depends on their specific characteristics. However, in general, the Wiener representation should be preferred when the system dynamics vary with the operating point. On the other hand, when only the system gain varies with the operating point, the Hammerstein model generally outperforms the Wiener representation [9].

The sigmoidal function $f(P_T)$ is specifically given as follows:

$$df(P_T)/dP_T = g(P_T) = ae^{\left(\frac{P_T}{b}\right)}\left(-\frac{P_T}{b}+1\right)u(-P_T) + ae^{\left(\frac{-P_T}{c}\right)}\left(\frac{P_T}{c}+1\right)u(P_T) \quad (1)$$

$$f(P_T) = ae^{\left(\frac{P_T}{b}\right)}(2b-P_T)u(-P_T) - \left[ae^{\left(\frac{-P_T}{c}\right)}(2c+P_T)+2a(b+c)\right]u(P_T). \quad (2)$$

Here, $g(P_T)$ is the unimodal arterial compliance curve and is defined by an exponential-linear function with $u(\cdot)$ representing the unit step function, parameter a indicating the function height at zero transmural pressure, and parameters b and c denoting the function widths over the negative and positive transmural pressure regimes [10]. For simplicity, the linear dynamics are represented with a unity gain single pole filter $H(s)$. The filter has one parameter (d) denoting its pole location. Fig. 3 shows the Hammerstein and Wiener viscoelastic models.

For comparison, a purely Elastic model was also employed. This model consists of just $f(P_T)$, as also shown in Fig. 3.

Note that the unknown k scale factor for mapping the unobserved $V(t)$ to the measured $PPG_{ac}(t)$ (Fig. 2) can be absorbed by the a parameter. So, the model parameters for estimation are $e = a \cdot k$, b, and c for all three models along with d for the Hammerstein and Wiener models.

D. *Model Fitting*

The parameters were estimated for each model and participant by fitting the estimated PPG_{ac} output of the model driven by the measured transmural pressure input to the measured PPG_{ac} output in the least squares sense. A trust-region optimization method [11], implemented with the Matlab

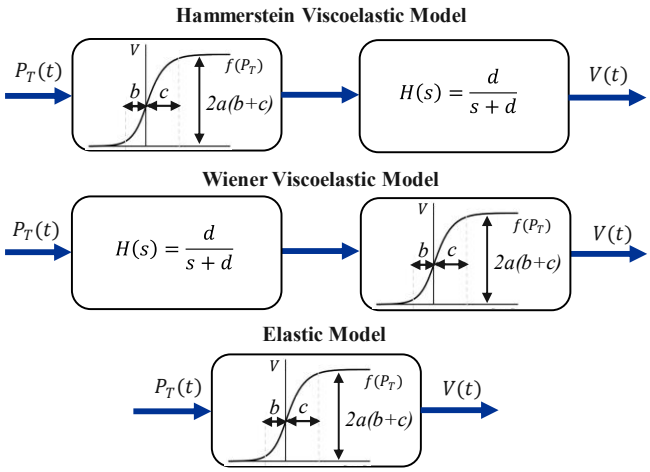

Fig. 3. Candidate finger artery viscoelastic and elastic models to represent the system for identification. All models include static sigmoidal nonlinearity with three unknown parameters defining the arterial compliance curve (a, b, and c). The viscoelastic models also include a unity gain single pole transfer function with another unknown parameter (d) defining its cutoff frequency. The cutoff frequency is inversely related to the extent of viscoelasticity. The unknown parameter k (Fig. 2) is absorbed with the a parameter.

fmincon function, was specifically applied to estimate e and d or e alone for each pair of b and c between 1 and 20 mmHg in unity increments. These parameter ranges encompass the typical parameter values for the brachial artery, which are expected to be larger than the parameter values for thin finger arteries [4], [5] (see Section IV.C). Then, the best fitting model was selected amongst the candidates. Although classic system identification tools could have been leveraged to estimate the d parameter for the Hammerstein model, such tools were not applicable to the Wiener model due to the unobservable $V(t)$. Therefore, the same estimation method was used for all models for a fair comparison.

Since volume-clamp devices can yield appreciable error in the mean value of the finger BP waveform [12], an offset to the mean value of the waveform was included as another parameter for estimation. This parameter was estimated through grid search from -10 to 10 mmHg in unity increments. This additional free parameter was required for satisfactory model fitting to the oscillograms.

E. Model Evaluation

Each model for each participant was evaluated in terms of the normalized root-mean-square-error of the PPG_{ac} fit (RMSE) and the normalized root-mean-square-error of the oscillogram fit ($RMSE_o$). The normalizing term is the root-mean-square of the measurement (PPG_{ac} or oscillogram) so that both errors have percent units. The measured oscillograms were computed as the peak-to-peak amplitude of the PPG_{ac} waveform followed by five-beat median filtering to mitigate measurement and respiratory artifacts. The errors for each model were statistically compared using the Wilcoxon signed rank test.

F. Model Simulations

To understand the impact of finger artery viscoelasticity on the BP computation, a model parametric sensitivity analysis was performed. The median of the parameter estimates of each participant and model was used for simulation. A simulated finger BP waveform $P_a(t)$ and a 60-second linear increase from 10 to 200 mmHg in finger pressure $P_e(t)$ were used to form the $P_T(t)$ input. $P_a(t)$ was constructed via a truncated Fourier series model as follows:

$$P_a = \mathrm{DP} + 0.5\mathrm{PP} + 0.36\mathrm{PP}\left(\sin(\omega t) + \frac{1}{2}\sin 2(\omega t) + \frac{1}{4}\sin(3\omega t)\right) \quad (3)$$

where ω is the angular frequency of heart rate, which was fixed at 60 beats per minute [13].

The output of the model, the simulated blood volume $V(t)$, was then highpass filtered. The oscillogram was constructed by plotting the simulated oscillation amplitudes (O_a) versus the simulated P_e. The finger pressures at minimum and maximum slopes of the simulated oscillogram ($P_{minslope}$, $P_{maxslope}$) were used to estimate SP and DP, respectively, as shown in Fig 4. This derivative algorithm is popular in oscillometry and can be particularly effective for finger arteries according to the elastic model [5] (see Section IV.D).

A number of simulations was performed to compute the sensitivity of the BP computation errors of the derivative algorithm to up to ±50% variations in the PP and b, c or d parameters.

III. Results

A. Model Comparisons – Representative Participant

Representative sample (median fitting error result) of estimated PPG_{ac} waveforms via the Wiener and the Elastic models are benchmarked against the measured PPG_{ac} waveform from a participant in Fig. 5. The plot demonstrates better agreement between the estimated and measured waveforms for the viscoelastic model (similar results were obtained with the Hammerstein model but not included for clarity). The following general observations can be made from the sample: (1) the viscoelastic model results in a smoother PPG_{ac} waveform (similar to the measured waveform) with more damped second and third waveform peaks, and (2) the PPG_{ac} amplitude at high finger pressure (toward the end of the waveform) is better represented by the viscoelastic model. For this participant, the RMSE values were 18.8%, 21.7%, and 46.9% for the Hammerstein, Wiener, and Elastic models, respectively.

The corresponding estimated and measured oscillograms are shown in Fig. 6. This plot shows that the Elastic model is not able to fit the oscillogram well to the right of the maximum oscillation amplitude, whereas the viscoelastic model captures the oscillation amplitude better. For this participant, the $RMSE_o$ values were 7.2%, 5.9%, and 13.6% for the Hammerstein, Wiener, and Elastic models, respectively.

B. Model Comparisons – All Participants

The model fitting errors of the estimated versus measured PPG_{ac} waveform computed across the 15 participants are shown in Fig. 7a. The plot includes data points representing the RMSE values for each participant. The RMSE values (median (interquartile range)) were 29.8% (26.9%-33.8%), 30.5% (25.6%-34.0%), and 50.9% (46.7%-53.7%) for the Hammerstein, Wiener, and Elastic models, respectively. The RMSE values of both viscoelastic models were significantly lower than the RMSE value of the Elastic model ($p < 0.01$). More importantly, the error was reduced by almost half, which means the one additional parameter in the viscoelastic models (d) was important in modeling the arterial transmural pressure – volume relationship and did not merely help in fitting noise.

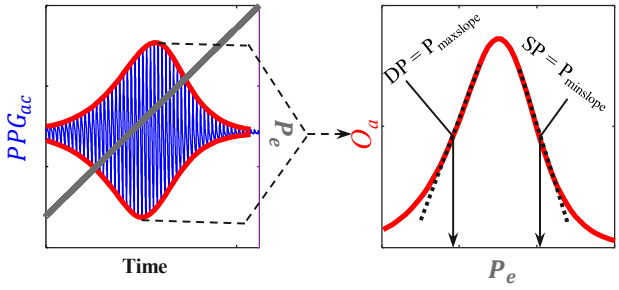

Fig. 4. Popular derivative algorithm for oscillometric BP computation [10] in model simulations. The external pressure (P_e) of an artery is swept while measuring the blood volume oscillations (PPG_{ac}). The oscillogram (O_a) is then formed as the function relating the peak-to-peak amplitude or envelope difference of PPG_{ac} to P_e. Systolic BP (SP) and diastolic BP (DP) are lastly estimated as the P_e at minimum and maximum oscillogram slopes.

This article has been accepted for publication in IEEE Transactions on Biomedical Engineering. This is the author's version which has not been fully edited and content may change prior to final publication. Citation information: DOI 10.1109/TBME.2024.3388316

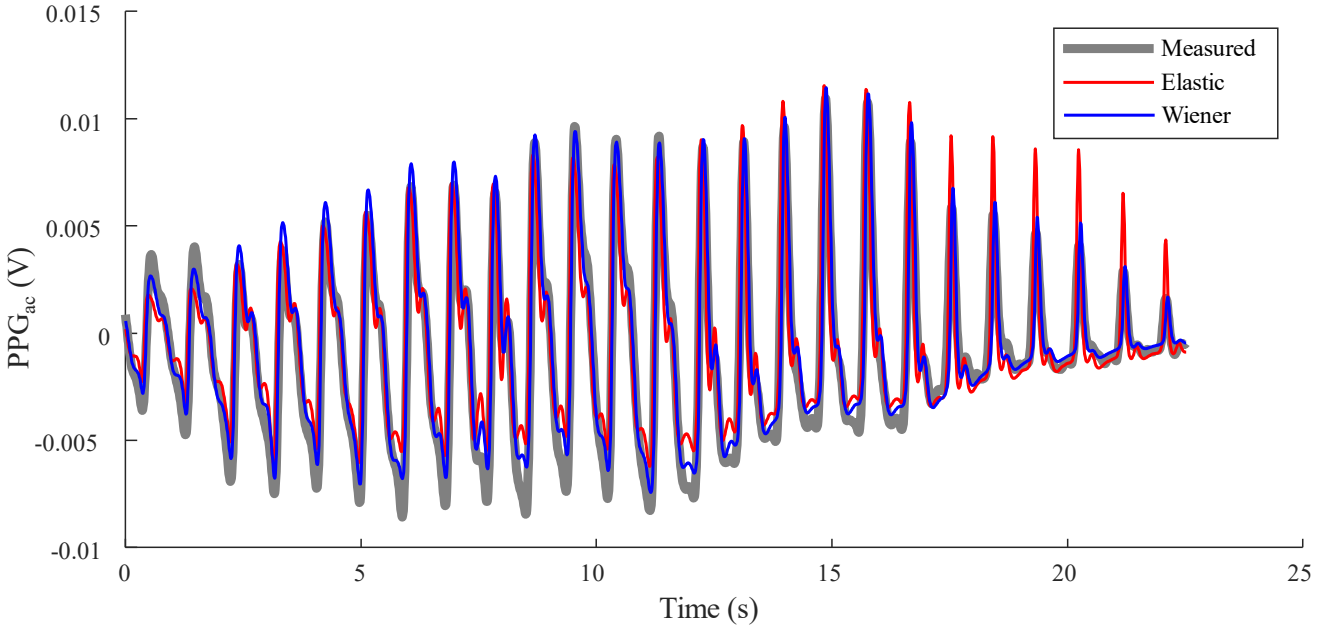

Fig. 5. Representative sample of model-estimated and measured PPG$_{ac}$ waveforms during finger pressing. The Hammerstein model yielded a similar estimated waveform to the Wiener model and is thus not shown.

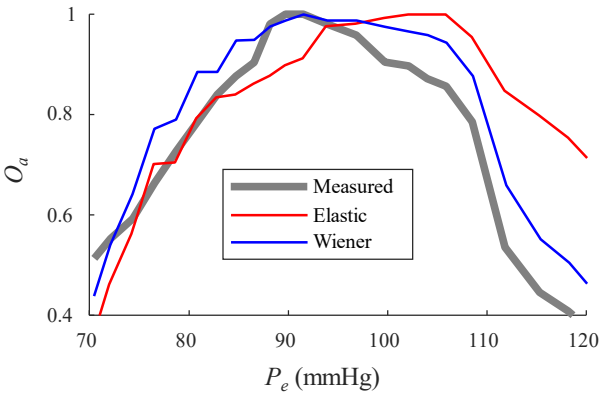

Fig. 6. Constructed oscillograms from the representative sample in Fig. 5. The oscillogram relates the peak-to-peak amplitude of the PPG$_{ac}$ waveform (O_a) to the corresponding P_e.

The corresponding model fitting errors of the estimated versus measured oscillograms are shown in Fig. 7b. The RMSE$_o$ values were 6.4% (5.0%-8.2%), 5.9% (4.5%-7.9%), and 13.6% (9.1%-17.5%) for the Hammerstein, Wiener, and Elastic models, respectively. The RMSE$_o$ values were significantly lower for both viscoelastic models ($p < 0.01$), and the error reduction was likewise about a half. While the RMSE$_o$ values for the two viscoelastic models were comparable, the RMSE$_o$ value for the Wiener model was statistically lower than the RMSE$_o$ value for the Hammerstein model ($p < 0.05$).

The estimated b and c model parameters for all participants are shown in Figs. 7c and 7d. The b and c parameters were not significantly different between the models and were about 8 and 12 mmHg, respectively.

The estimated d model parameter of the viscoelastic models for all participants is shown in terms of transfer function cutoff frequency in Fig. 7e. For both models, the cutoff frequency was about 3 Hz, indicating a significant damping effect.

The viscoelastic models thus fit the measurements much better than the Elastic model. However, while the Wiener model did yield lower oscillogram fitting error than the Hammerstein model, the two models produced similar results overall.

Toward a further comparison to distinguish between the viscoelastic models, Fig. 8 shows the simulated oscillograms from all three models with median parameter values when

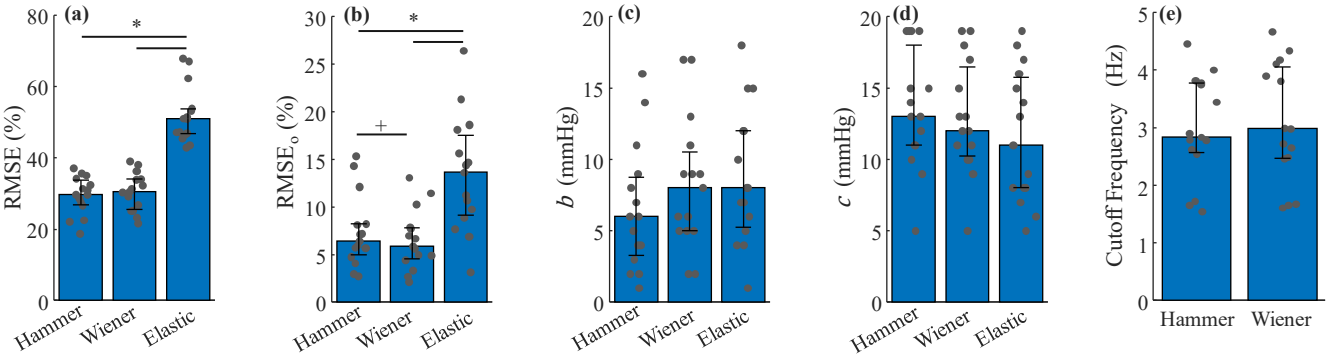

Fig. 7. Overall fitting errors and parameter estimates (N=15). (a) Root-mean-square-error of the estimated PPG$_{ac}$ waveform (RMSE) in percent, **(b)** root-mean-square-error of the constructed oscillogram (RMSE$_o$) in percent **(c)-(e)** b parameter, c parameter, and d parameter in terms of transfer function cutoff frequency. Bars represent median±quartiles, and data points represents individual participants. *p<0.01, +p<0.05.

This article has been accepted for publication in IEEE Transactions on Biomedical Engineering. This is the author's version which has not been fully edited and content may change prior to final publication. Citation information: DOI 10.1109/TBME.2024.3388316

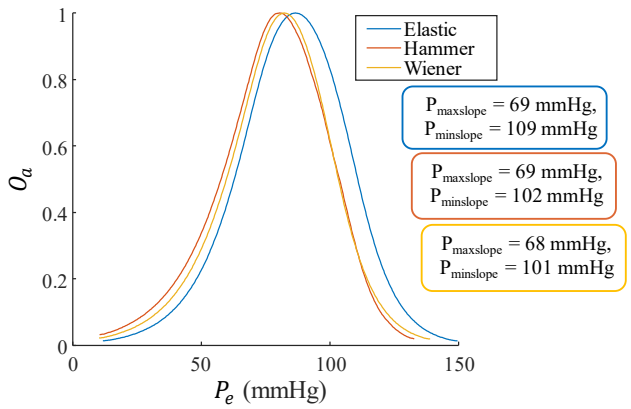

Fig. 8. Simulated oscillograms via the models with median parameter values and SP = 110 mmHg and DP = 70 mmHg. $P_{minslope}$ and $P_{maxslope}$ (P_e at minimum and maximum oscillogram slopes) are popular and Elastic model-based estimates of systolic BP (SP) and diastolic BP (DP), respectively.

driven with a simulated transmural pressure waveform. The oscillograms via the viscoelastic models were compressed compared to the Elastic model. If the Hammerstein model with linear dynamics following the static nonlinearity were better, first deconvolving the estimated linear transfer function from the PPG_{ac} waveform and then constructing the oscillogram would yield an oscillogram that is expanded much like the simulated oscillogram via the Elastic model. On the other hand, if the Wiener model were better, such deconvolution may have less impact on the oscillogram due to the linear dynamics preceding the static nonlinearity.

Fig. 9a shows experimental oscillograms from a representative participant. The plot specifically displays the constructed oscillogram from the original measured PPG_{ac} waveform and the oscillogram after deconvolving the waveform with the estimated transfer function. The deconvolution had little impact on the oscillogram. For comparison, Figs. 9b and 9c show the analogous results for simulated PPG_{ac} waveforms with the Wiener and Hammerstein models, respectively. The participant's estimated model parameters (a, b, c and d) and measured BP and heart rate were used for the simulations. Very similar results are observed for the experimental data and the Wiener model simulation; the oscillogram remains similar after deconvolution. On the other hand, as just explained, deconvolution stretched the oscillogram simulated with the Hammerstein model (i.e., the deconvolution canceled out the effect of damping).

In sum, the Wiener model explains the oscillometric finger pressing data better than the Hammerstein model and much better than the Elastic model.

C. Wiener Model Parametric Sensitivity Analysis

The model simulations with median parameter values indicate that viscoelasticity causes the popular derivative algorithm to underestimate SP via $P_{minslope}$ but barely affects this algorithm in computing DP via $P_{maxslope}$ (Fig. 8).

A parametric sensitivity analysis of the BP estimation errors of the derivative algorithm was performed via further simulations with the Wiener model. Fig. 10a shows the SP estimation errors as a function of PP for different transfer function cutoff frequencies. The underestimation of SP via $P_{minslope}$ increases with increasing PP and decreasing cutoff frequency (i.e., greater viscoelasticity). Fig. 10b shows that the b parameter only slightly affects the SP estimation error. Figs. 10c and 10d show the DP estimation errors via $P_{maxslope}$ as a function of PP for different transfer function cutoff frequencies and for different c parameters, respectively. These parameters affect the DP computation relatively little.

In sum, finger artery viscoelasticity causes the derivative algorithm to underestimate SP. The SP underestimation is substantial when both PP and the extent of viscoelasticity are large.

D. Potential Estimation of the Transfer Function Cutoff Frequency to Compensate for Finger Artery Viscoelasticity

Quantifying the extent of finger artery viscoelasticity from existing measurements could help compensate for its adverse effect on the BP computation. The mean of the normalized PPG_{ac} waveform at the maximum oscillation beat (PPG_{mean}) is a good candidate, as the sigmoidal function may be most linear at zero transmural pressure where the maximum oscillation typically occurs. Therefore, the relationship between arterial volume and pressure may be close to the transfer function alone. Assuming relatively little variability in the finger BP waveform between individuals, PPG_{mean} should be large when the

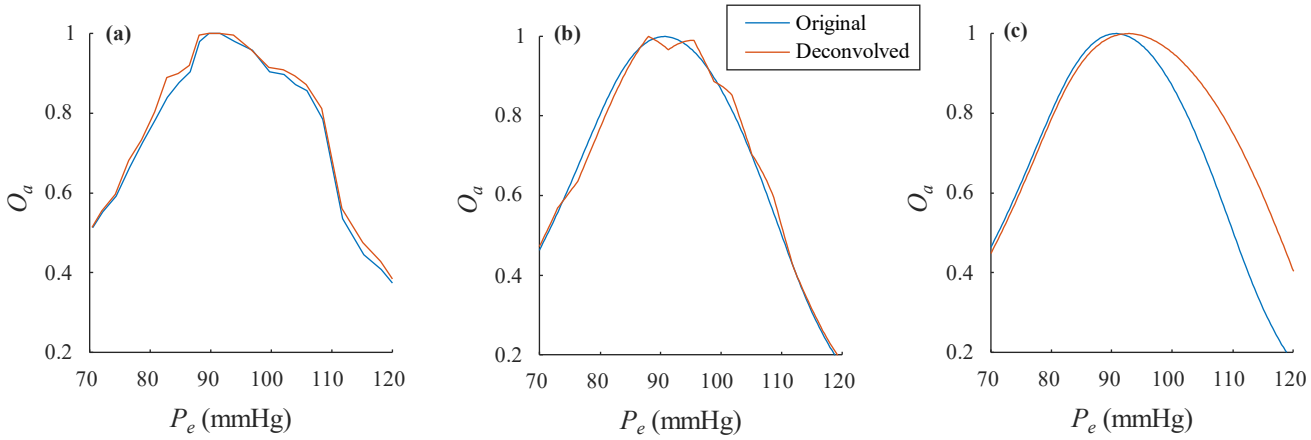

Fig. 9. Representative oscillograms constructed from the original PPG_{ac} waveform and the deconvolved PPG_{ac} waveform. (a) Measurements from a participant, **(b)** Wiener model simulations, and **(c)** Hammerstein model simulations. Deconvolution was performed using the estimated transfer function of the participant, and simulations were performed using the participant's model parameter estimates and measurements.

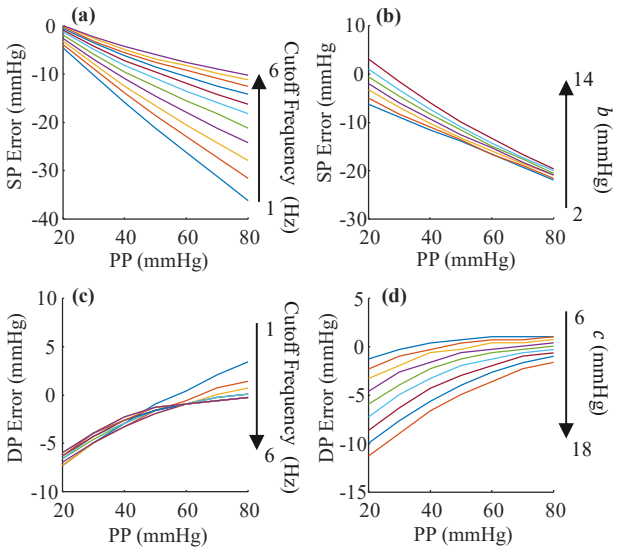

Fig. 10. BP computation errors of the derviative algorithm as a function of model parameters via simulations with the Wiener model. (a)-(b) SP errors via $P_{minslope}$ and **(c)-(d)** DP errors via $P_{maxslope}$**.** Each parameter was varied by ±50% relative to median values (Fig. 7) in this parametric sensitivity analysis.

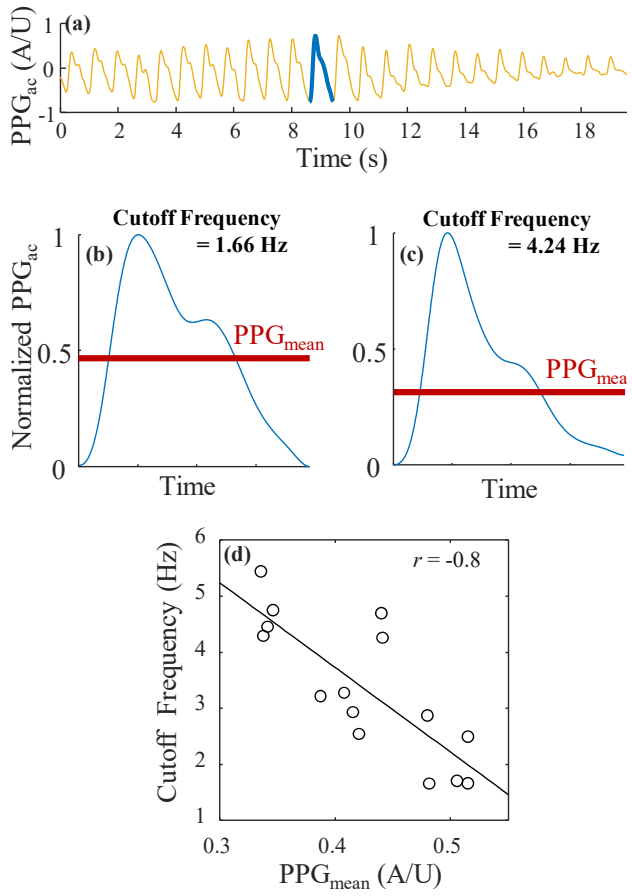

Fig. 11. PPG_{mean} correlates with the transfer function cutoff frequency. (a) PPG_{mean} is extracted from the PPG_{ac} waveform at maximum oscillation. The extracted beat is normalized from 0 to 1 in amplitude, and the mean of the beat is then computed. **(b)-(c)** Two representative samples of PPG_{mean} along with the estimated transfer function cutoff frequency. **(d)** Overall correlation plot between the cutoff frequency and PPG_{mean}. *r* is Pearson correlation coefficient.

viscoelastic effect is large (largely damped; "bulky PPG oscillation") and small when there is little viscoelasticity (purely elastic; "spiky PPG oscillation").

Fig. 11a shows an example of the PPG_{ac} waveform with the maximum oscillation beat highlighted. Figs. 11b and 11c show two representative examples from different participants of the PPG_{ac} waveform at the maximum oscillation beat after amplitude normalization from 0 to 1. When the transfer function cutoff frequency of the Wiener model is low, the PPG oscillation is bulky (Fig. 11b). When the cutoff frequency is higher, the PPG oscillation is sharper (Fig. 11c). Fig. 11d shows that PPG_{mean} correlates well with the Wiener model cutoff frequency over all participants (r = -0.8).

IV. Discussion

The oscillometric finger pressing method is a potential method for calibration-free cuffless BP monitoring via widely available smartphones [2], [3]. While the oscillometric principle is proven for brachial artery BP measurement, small finger arteries are more viscoelastic, which could make computing BP from finger oscillometric measurements more challenging.

A. Importance of Finger Artery Viscoelasticity

In this study, we conducted nonlinear viscoelastic modeling in the context of the oscillometric finger pressing method. We first compared viscoelastic and purely elastic models in terms of fitting experimental data. We specifically fitted the output of each model to a measured transmural pressure input to the measured PPG_{ac} waveform during finger pressing from 15 participants. We found that Hammerstein and Wiener viscoelastic models could fit the data with half the error of the Elastic model (Figs. 7a and 7b). These system identification results indicate that finger artery viscoelasticity should be accounted for in the oscillometric finger pressing method.

B. Wiener Model of Viscoelasticity

Although the Hammerstein and Wiener models are quite similar in their architecture, which may explain why both models fitted the data similarly, we found that the Wiener model was more representative of finger artery viscoelasticity. This model was better in fitting oscillogram data (Fig. 7b) and in predicting the effect of deconvolution on the oscillogram data (Fig. 9). Moreover, we found that the Wiener model has a physical correspondence; that is, it is equivalent to a nonlinear Voigt model of viscoelasticity, as shown in Fig. 12.

The linear Voigt model is the simplest of the physical models of viscoelasticity. It compresses like a purely elastic spring with slow deformation but offers additional resistance to fast deformation via a damper (i.e., it acts as a lowpass filter). The model is a purely viscous dashpot and a purely elastic spring connected in parallel.

We modified the Voigt model for nonlinear arteries. In the modification, we treated pressure like force and volume as length.

First, we employed a nonlinear spring, where the reaction pressure applied by the spring is the inverse sigmoidal arterial volume-pressure relationship (see Eqs. (1) and (2)) as follows:

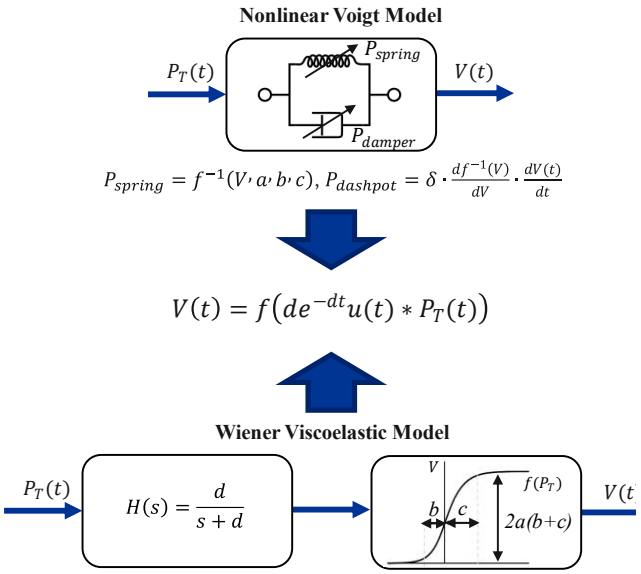

Fig. 12. Equivalence of the best-fitting Wiener model to a physical model of oscillometric finger pressing measurements. The physical model is a nonlinear Voigt model with a constant pole when linearized around any arterial volume.

$$P_{spring}(t) = f^{-1}(V(t), a, b, c). \tag{4}$$

The spring constant or volume elastance may thus be given as follows:

$$k = \frac{dP_{spring}}{dV} = \frac{df^{-1}(V)}{dV} \tag{5}$$

Second, we employed a nonlinear dashpot. We defined the nonlinearity so that the linearized Voigt model at any arterial volume has a constant transfer function pole (see below for justification). In other words, the damping coefficient η increases proportionally with k. The reaction pressure applied by the dashpot is therefore given as follow:

$$\begin{aligned} P_{dashpot}(t) &= \eta \cdot \frac{dV(t)}{dt} = \delta \cdot k \cdot \frac{dV(t)}{dt} \\ &= \delta \cdot \frac{df^{-1}(V)}{dV} \cdot \frac{dV(t)}{dt} \end{aligned} \tag{6}$$

where δ is a free parameter of the model.

Putting everything together, the following first-order nonlinear differential equation is obtained:

$$P_T(\mathrm{t}) = f^{-1}\big(V(t)\big) + \delta \cdot \frac{df^{-1}\big(V(t)\big)}{dt}. \tag{7}$$

This equation can be solved for $V(t)$ as follows:

$$V(t) = f(de^{-dt}u(t) * P_T(t)), \tag{8}$$

where $d = 1/\delta$, $u(t)$ is again the unit step function, and $*$ is the convolution operation. Eq. 8 is equivalent to the Wiener model with a unity gain single pole transfer function and static sigmoidal nonlinearity (Fig. 12).

The physical correspondence between the Wiener model and nonlinear Voigt model here assumes a constant pole. This assumption may be justified by the *ex vivo* study of rabbit aortic strips by Wurzel *et al.* [14]. These investigators used a standard linear solid model of arterial viscoelasticity, wherein the transfer function has one pole and one zero. Their data indicate that the model parameters vary with external force applied to the artery (or pre-stretch). However, the pole of the model transfer function remains constant over the range of stretches. The constant pole is a necessary condition for the Wiener model's physical correspondence to the nonlinear Voigt model.

We tried to add a zero to the transfer function in this study, but it did not improve the model fitting. The different dynamics observed herein may be due to numerous differences such as the tested artery (finger vs aorta), the tested subject (human vs rabbit), or the artery environment (*in vivo* vs *ex vivo*).

C. *Wiener Model Parameter Values*

The Wiener model parameters b and c indicate the widths of the arterial compliance curve over the negative and positive transmural pressure regimes, respectively. The b parameter is expected to be small for collapsible finger arteries, whereas the ratio of the b and c parameters may be similar to the brachial artery [5]. The b and c values for the finger arteries in this study were 8.0 (5-10.5) and 12.0 (10.3-16.5) mmHg (Figs. 7c and 7d). In comparison, the b and c parameter values for the brachial artery in cardiac catheterization patients with stiffer arteries are 11 and 17 mmHg [4]. While the finger artery parameters are smaller than their brachial artery counterparts and the b to c ratios are similar, we had expected the b parameter for the finger artery to be even smaller (e.g., < 5 mmHg). One potential reason for the higher b parameter values could be inaccuracy of the volume-clamp device in measuring the input finger BP waveform. For instance, if SP were underestimated by the device, the model would have to increase b to compensate [10]. Also note that there was large variability in the b and c parameters (Figs. 7c and 7d).

The Wiener model transfer function cutoff frequency, which may be readily computed from the d parameter, is inversely related to the extent of finger artery viscoelasticity. The transfer function cutoff frequency value was 3.0 (2.5-4.0) Hz (Fig. 7e). This cutoff frequency is close to the typical heart rates (1-2 Hz). For further comparison, the population average transfer function from brachial to finger BP shows a resonance peak at 7 Hz [15]. This difference additionally underscores the significant impact finger artery viscoelasticity can have on the oscillometric BP computation. Note that the transfer function cutoff frequency is necessarily higher than the cutoff frequency of the highpass filter used to extract $PPG_{ac}(t)$. In the end, the overall dynamics relating $P_T(t)$ (transmural pressure) to $PPG_{ac}(t)$ (blood volume oscillations) exhibit nonlinear bandpass characteristics.

D. *Wiener Model Simulations*

We performed a parametric sensitivity analysis with the Wiener model to illustrate the impact of finger artery viscoelasticity on the derivative algorithm for computing BP (see Fig. 4). Our analysis showed that (1) SP computation via $P_{minslope}$ is much more affected by viscoelasticity than DP

computation via $P_{maxslope}$ and (2) PP and the transfer function cutoff frequency are the major contributors to the SP underestimation (Fig. 10). This sensitivity analysis is supported by our previous experimental results where PP tended to be underestimated by the derivative algorithm [5], [6].

We chose the derivative algorithm, because we previously showed that this popular algorithm can yield BP with minimal error for purely elastic, collapsible finger arteries and in the absence of noise [5]. Any significant error of the derivative algorithm in the model simulations would thus be due to viscoelasticity alone. However, we expect that these results would apply to other popular oscillometric algorithms, which typically do not take viscoelasticity into account. For instance, we applied the fixed ratio algorithm with 0.85 and 0.55 for the DP and SP ratios, respectively [10], and found similar results (not shown).

The nonlinear Voigt model helps in understanding these results. In this model, the damping reaction pressure is proportional to the damping coefficient and the time rate of change of the artery volume (Eq. 6). Therefore, for a given artery volume elastance and heart rate, large PP would result in large rate of change in artery volume, resulting in a more damped volume waveform. Since damping affects the oscillogram more at high finger pressures due to the sharper volume waveform at these pressures [5], SP computation is most affected by viscoelasticity. It is important to note that the rate of change in arterial volume can be affected by the shape of the waveform (not only its amplitude, i.e., PP), which was kept constant in the simulations. Heart rate was also kept constant in the simulations but will have a similar effect on the damping reaction pressure. For instance, increased heart rate will proportionally increase the damping leading to the same effect as PP on BP computation algorithms. A particularly important feature for the underestimation of SP may be the finger BP upstroke time. In this study, the sensitivity analysis was kept simple by using only PP to express the shape of the input to the model.

E. Potential Remedies to Compensate for the Adverse Effects of Finger Artery Viscoelasticity

We lastly explored potential remedies to compensate for the adverse effects of finger artery viscoelasticity in the BP computation. We found that the PPG_{ac} waveform shape can provide information about the system characteristics. More precisely, it can provide an estimation of the cutoff frequency of the transfer function (Fig. 11). We specifically showed that PPG_{mean} – the average of the normalized PPG_{ac} waveform at the maximum oscillation beat – correlates well with the transfer function cutoff frequency (r = -0.8). Although the mean value was employed here, any metric representing bulkiness could be used including the root-mean-square (r = -0.83, not shown). These markers could be used as input to an algorithm to compensate for BP computation error caused by viscoelasticity. For instance, they could be used directly as input (along with other features extracted from the oscillometric finger pressing data) to a machine learning model to compute SP and DP. Another example is to use the model to compensate for the error in popular algorithms (e.g., derivative algorithm). For instance, for a given algorithm, a mapping from PP estimate and cutoff frequency to BP error (Fig. 10) can be created using training data comprising oscillometric finger pressing data and reference cuff BP. Then, for a given finger pressing measurement, PP is computed (e.g., via the derivative algorithm), the cutoff frequency is estimated (e.g., via PPG_{mean}), and the BP error can thus be calculated via the aforementioned mapping.

We used deconvolution herein as a method to distinguish the Wiener model from the Hammerstein model and show that actual finger pressing data display similar behavior to the Wiener model (Fig. 9). Even though deconvolution of the PPG_{ac} waveform may not be able to remove viscoelastic effects from the oscillogram, it can still provide an estimate of the BP waveform shape. In fact, deconvolving the PPG_{ac} waveform beat at maximum oscillation with the estimated transfer function may provide an accurate BP waveform shape, since the sigmoidal function is approximately linear at around the maximum oscillation. This beat could be used in advanced algorithms to compute BP. For instance, features from the derived beat could be used as input to a machine learning model to compute BP. Alternatively, an absolute BP waveform beat may be determined using deconvolution. First, a popular algorithm is applied to compute SP and DP. Then, the PPG_{ac} waveform beat at maximum oscillation is calibrated to these BP levels. Next, the transfer function with estimated cutoff frequency is deconvolved from the beat. Finally, the maximum and minimum of the deconvolved beat are detected to arrive at SP and DP corrected for finger artery viscoelasticity.

A significant weakness of pure PPG markers of viscoelasticity is that the bulkiness of the normalized PPG_{ac} waveform at the maximum oscillation beat reflects both the transfer function cutoff frequency and the input finger BP waveform. Therefore, a change in the BP waveform (due to, e.g., aging) may erroneously be interpreted as a change in the system viscoelasticity. Nevertheless, at least in this study, viscoelasticity was a prominent contributor to PPG_{mean}. It is also possible that viscoelastic effects are more important in determining PPG bulkiness in general.

F. Limitations

The main limitation of this study was the assumption that the volume-clamp device gave an accurate shape for the finger BP waveform input to the model. On the other hand, making this assumption was necessary just to be able to investigate finger artery viscoelasticity. Also, our current oscillometric finger pressing data are from mostly normotensive users with reference BP obtained using an automatic cuff device. However, large PP is required to validate the potential remedies so that the estimation error due to viscoelasticity is significantly larger than the reference BP measurement error. The evaluation of the potential remedies for more accurate oscillometric BP computation must therefore be left for future work. A potential avenue to minimize measurement error would be to employ manual auscultation for the reference cuff BP measurements. The difference in finger and arm BP measurements, which could potentially be accounted for by using a transfer function [15], must likewise be left for subsequent investigation.

V. Conclusion

We investigated whether finger artery viscoelasticity must be taken into account in the context of oscillometric finger pressing method for potential cuffless BP monitoring and, if so, how viscoelasticity affects the oscillometric BP computation. We developed nonlinear viscoelastic models and fitted the models to oscillometric finger pressing data. We found that a Wiener viscoelastic model, consisting of a first-order linear transfer function followed by a static sigmoidal function, fitted the data much better than a purely elastic model, thereby indicating significant effect of viscoelasticity in oscillometric finger pressing. We also showed that the Wiener model explained the data better than a Hammerstein viscoelastic model and carries physical meaning. Through simulations with the Wiener model, we observed that viscoelasticity leads to mild misestimation of DP but large underestimation of SP when using a popular oscillometric BP computation algorithm. The SP underestimation increases with both PP and the inverse of the transfer function cutoff frequency, which is an index of arterial viscoelasticity. Although viscoelasticity negatively impacts BP computation algorithms, we discovered PPG waveform markers of the transfer function cutoff frequency, which could potentially be used for enhancing BP computation accuracy without additional sensors. This work improved our understanding of finger artery viscoelasticity in the context of the oscillometric finger pressing method and may be an important step toward improving hypertension awareness and control via smartphone-based BP monitoring.

References

[1] B. Zhou *et al.*, "Worldwide Trends in Hypertension Prevalence and Progress in Treatment and Control from 1990 to 2019: A Pooled Analysis of 1201 Population-Representative Studies with 104 Million Participants," *The Lancet*, vol. 398, no. 10304, pp. 957–980, Sep. 2021, doi: 10.1016/S0140-6736(21)01330-1.

[2] A. Chandrasekhar, C.-S. Kim, M. Naji, K. Natarajan, J.-O. Hahn, and R. Mukkamala, "Smartphone-Based Blood Pressure Monitoring Via the Oscillometric Finger-Pressing Method," *Sci. Transl. Med.*, vol. 10, no. 431, p. eaap8674, Mar. 2018, doi: 10.1126/scitranslmed.aap8674.

[3] R. Mukkamala, G. S. Stergiou, and A. P. Avolio, "Cuffless Blood Pressure Measurement," *Annu. Rev. Biomed. Eng.*, vol. 24, no. 1, pp. 203–230, 2022, doi: 10.1146/annurev-bioeng-110220-014644.

[4] V. Dhamotharan *et al.*, "Mathematical Modeling of Oscillometric Blood Pressure Measurement: A Complete, Reduced Oscillogram Model," *IEEE Trans. Biomed. Eng.*, vol. 70, no. 2, pp. 715–722, Feb. 2023, doi: 10.1109/TBME.2022.3201433.

[5] M. Freithaler, A. Chandrasekhar, V. Dhamotharan, C. Landry, S. G. Shroff, and R. Mukkamala, "Smartphone-Based Blood Pressure Monitoring via the Oscillometric Finger Pressing Method: Analysis of Oscillation Width Variations Can Improve Diastolic Pressure Computation," *IEEE Trans. Biomed. Eng.*, pp. 1–11, 2023, doi: 10.1109/TBME.2023.3275031.

[6] C. Landry, V. Dhamotharan, A. Chandrasekhar, S. G. Shroff, and R. Mukkamala, "A Smartphone Application to Detect and Control Systolic Hypertension in the Underserved," *Submitted*.

[7] G. J. Langewouters, A. Zwart, R. Busse, and K. H. Wesseling, "Pressure-Diameter Relationships of Segments of Human Finger Arteries," *Clin. Phys. Physiol. Meas.*, vol. 7, no. 1, p. 43, Feb. 1986, doi: 10.1088/0143-0815/7/1/003.

[8] I. W. Hunter and M. J. Korenberg, "The Identification of Nonlinear Biological Systems: Wiener and Hammerstein Cascade Models," *Biol. Cybern.*, vol. 55, no. 2, pp. 135–144, Nov. 1986, doi: 10.1007/BF00341929.

[9] L. A. Aguirre, M. C. S. Coelho, and M. V. Corrêa, "On the interpretation and practice of dynamical differences between Hammerstein and Wiener models," *IEE Proc. - Control Theory Appl.*, vol. 152, no. 4, pp. 349–356, Jul. 2005, doi: 10.1049/ip-cta:20045152.

[10] A. Chandrasekhar *et al.*, "Formulas to Explain Popular Oscillometric Blood Pressure Estimation Algorithms," *Front. Physiol.*, vol. 10, 2019, Accessed: Feb. 23, 2022. [Online]. Available: https://www.frontiersin.org/article/10.3389/fphys.2019.01415

[11] R. H. Byrd, J. C. Gilbert, and J. Nocedal, "A Trust Region Method Based on Interior Point Techniques for Nonlinear Programming," *Math. Program.*, vol. 89, no. 1, pp. 149–185, Nov. 2000, doi: 10.1007/PL00011391.

[12] R. Mukkamala, J.-O. Hahn, and A. Chandrasekhar, "11 - Photoplethysmography in Noninvasive Blood Pressure Monitoring," in *Photoplethysmography*, J. Allen and P. Kyriacou, Eds., Academic Press, 2022, pp. 359–400. doi: 10.1016/B978-0-12-823374-0.00010-4.

[13] C. F. Babbs, "Oscillometric Measurement of Systolic and Diastolic Blood Pressures Validated in a Physiologic Mathematical Model," *Biomed. Eng. OnLine*, vol. 11, no. 1, p. 56, Aug. 2012, doi: 10.1186/1475-925X-11-56.

[14] M. Wurzel, G. R. Cowper, and J. M. McCooK, "Smooth Muscle Contraction and Viscoelasticity of Arterial Wall," *Can. J. Physiol. Pharmacol.*, vol. 48, no. 8, pp. 510–523, Aug. 1970, doi: 10.1139/y70-079.

[15] P. Gizdulich and K. H. Wasseling, "Reconstruction Of Brachial Arterial Pulsation From Finger Arterial Pressure," in *[1990] Proceedings of the Twelfth Annual International Conference of the IEEE Engineering in Medicine and Biology Society*, Nov. 1990, pp. 1046–1047. doi: 10.1109/IEMBS.1990.691590.